Alternating Ferromagnetic−Antiferromagnetic Interactions in a Manganese(II)−Azido One-Dimensional Compound: $[Mn(bipy)(N_3)_2]$

Roberto Cortés,[†,‡] Marc Drillon,[§] Xavier Solans,[⊥] Luis Lezama,[†] and Teófilo Rojo*[,†]

Departamento de Química Inorgánica, Universidad del País Vasco, Aptdo. 644, E-48080 Bilbao, Spain, Groupe des Materiaux Inorganiques, IPCMS, 67037 Strasbourg Cedex, France, and Departamento de Cristal-lografía, Universidad de Barcelona, 08028 Barcelona, Spain

Received August 21, 1996[⊗]

An alternating di-(μ-(end-on)azido)−di-(μ-(end-to-end)azido) manganese(II) one-dimensional compound, with formula $[Mn(bipy)(N_3)_2]$ (bipy = 2,2′-bipyridine), has been synthesized and characterized. Its crystal structure has been solved at room temperature. The complex crystallizes in the triclinic $P\bar{1}$ space group, with $a = 7.547(2)$ Å, $b = 9.137(4)$ Å, $c = 9.960(4)$ Å, $\alpha = 110.76(4)°$, $\beta = 104.43(2)°$, $\gamma = 100.41(3)°$, and $Z = 2$. The structure consists of manganese chains in which the Mn^{II} ions are alternatively bridged by two end-on (EO) and two end-to-end (EE) azido bridges. Each Mn^{II} ion has an octahedral coordination, completed by the two nitrogen atoms of the bipy ligand. The EO and EE bridges are arranged *cis*. This constitutes the first example of such an azido bridge chain for any metallic ion. ESR measurements show signals corresponding to $\Delta Ms = 1$ and $\Delta Ms = 2$ transitions, with no significant variations by modifying the temperature. The thermal variation of molar susceptibility reveals the existence of alternating ferro- and antiferromagnetic interactions, through alternating EO and EE azido bridges, in the compound. A theoretical model has been developed for an $S = {}^5/_2$ alternating ferromagnetic−antiferromagnetic coupled 1D system: the exchange parameters obtained with this model, considering the spin Hamiltonian $H = -J_1\sum S_{2i}S_{2i+1} - J_2\sum S_{2i+1}S_{2i+2}$, are $J_1 = 13.8$ K, $J_2 = -17.01$ K with g fixed at 2.0. Extended Hückel calculations are discussed to model the end-on and end-to-end bridged systems.

Introduction

In the past 2 decades, magnetic systems extending in one-dimension (1D) have been widely investigated from both experimental and theoretical viewpoints.[1] One of the reasons is that these systems provide excellent examples on which the development of suitable theoretical models affords a better understanding of the exchange interaction in extended lattices. As a result, new classes of molecular magnetic materials, often displaying low-dimensional structures, have been discovered which require the development of new theoretical models in order to correlate crystal and molecular structures with magnetic properties. In this area, studies of antiferromagnetic alternating chains have been particularly fruitful.[2] The regular alternation of the two antiferromagnetic J_i and J_{i+1} coupling constants occurring in this kind of system is achieved either by alternating the bridging ligands between the metal ions in a ...−L−M−L′−M−L−... sequence or by alternating spacing. The first method constitutes the safe synthetic route based on the coordinating capability of the bridging ligands, while the second one is a more hazardous procedure.

The large number of antiferromagnetic alternating chains contrasts with the paucity of alternating chains with J_i and J_{i+1} of different signs (ferro- and antiferromagnetic). In this work, we focus on systems containing simultaneously ferro- and antiferromagnetic exchange interactions. Several examples of this kind have recently been reported in both organic and inorganic chemistries,[3] all of them with $S = {}^1/_2$, for which a theoretical model has been proposed.[4] However, systems with $S > {}^1/_2$ have not yet been experimentally or theoretically described so far. There are at least two reasons justifying the theoretical effort in this way: (1) Often these systems have controversial ground states which depend on the relative magnitude and topology of the exchange interactions.[5] (2) A detailed knowledge of the value of the two exchange parameters and the subsequent correlation with structure is of particular importance in the design and construction of new high-spin polymers.[6]

The difficulties found in the synthesis of these systems are associated with both the design of ferromagnetically coupled dimers[7] and their polymerization through bridging ligands which mediate interdimer antiferromagnetic coupling. In this way, during the past years we have paid attention to the role played by pseudohalide ions, in particular azido ones, in bridging different transition metal ions in order to obtain polynuclear systems with ferromagnetic type interactions. Pseudohalide ions are able to bridge to the metal ions in several manners, including

† Departamento de Química Inorgánica, Universidad del País Vasco.
‡ Facultad de Farmacia. Universidad del País Vasco.
§ IPCMS Strasbourg.
⊥ Universidad de Barcelona.
⊗ Abstract published in *Advance ACS Abstracts,* January 15, 1997.

(1) (a) *Extended Linear Chain Compounds*; Miller, J. S., Ed.; Plenum: New York, 1983; Vol. 3. (b) Bonner, J. C. In *Magneto-structural Correlations in Exchange Coupled Systems*; Willet, R. D., Gatteschi, D., Kahn, O., Eds.; NATO ASI Series 140; Reidel: Dordrecht, The Netherlands, 1985; p 157. (c) *Magnetic Molecular Materials*; Gatteschi, D., Kahn, O., Miller, J. S., Palacio, F., Eds.; NATO ASI Series 198; Plenum: New York, 1991.
(2) Landee, C. P. In *Organic and Inorganic Low-Dimensional Crystalline Materials*; Delhaes, P., Drillon, M., Eds.; NATO ASI Series 168; Plenum: New York, 1987; p 75.
(3) (a) De Groot, H. J. M.; de Jongh, L. J.; Willet, R. D.; Reedijk, J. *J. Appl. Phys.* **1982**, *53*, 8038. (b) Benelli, C.; Gatteschi, D.; Carnegie, D. W.; Carlin, R. L. *J. Am. Chem. Soc.* **1985**, *107*, 2560. (c) de Munno, G.; Julve, M.; LLoret, F.; Faus, J.; Verdaguer, M.; Caneschi, A. *Angew. Chem., Int. Ed. Engl.* **1993**, *32*, 1046. (d) Vasilevesky, I.; Rose, N. R.; Stenkamp, R.; Willet, R. D. *Inorg. Chem.* **1991**, *30*, 4082.
(4) Borras-Almenar, J. J.; Coronado, E.; Curely, J.; Georges, R.; Gianduzzo, J. C. *Inorg. Chem.* **1994**, *33*, 5171.
(5) The typical situation is found in a chain of triangles as a consequence of spin frustration effects.
(6) Matsumoto, T.; Koga, N.; Iwamura, H. *J. Am. Chem. Soc.* **1992**, *114*, 5448.
(7) Kahn, O. *Comments Inorg. Chem.* **1984**, *3*, 105.

S0020-1669(96)01017-8 CCC: $14.00

end-to-end (EE) or *end-on* (EO) modes. The first type of bridge is known to favor antiferromagnetic interactions between the metal centers.[8] However, both the azide and cyanate anions in their end-on coordination mode have been shown to be able to promote ferromagnetic type interactions,[9] even for the manganese(II) ion with $S = {}^5/_2$.[10] As a result, the first azide[11] and cyanate[12] nickel(II) dinuclear compounds having this kind of bridging have been obtained and characterized. Furthermore, a synthetic strategy has successfully been achieved to obtain these types of compounds with ferromagnetic exchange coupling.[13]

To date, dinuclear,[14a,b] tetranuclear,[14c] and one-dimensional (1-D) polymeric systems,[14b] with EO bridges, together with dinuclear complexes[15a] and 1-D polymeric systems[15b−d] with EE bridges, have been synthesized. A two-dimensional (2-D) complex containing both EE and EO forms[16] has also been characterized.

The different magnetic behavior originated by the two kinds of azido bridges[10,17−19] could allow the formation of 1-D systems with alternating ferro- (through EO bridges) and antiferromagnetic (through EE bridges) exchanges, which are very scarce.[3] They could be prepared by synthesizing, considering some serendipity role, an adequate compound containing both types of bridging azides. With this aim in mind we have developed a synthetic method using the bidentate ligand 2,2′-bipyridine (bipy) with a metal/bidentate ligand 1:1 ratio. In this way, the four coordination vacancies around the metal ion should be completed by the excess of the azido ligands. Following this procedure, we have successfully isolated a novel doubly EO and doubly EE alternating Mn(II) chain with the empirical formula $[Mn(N_3)_2(bipy)]_n$ (bipy = 2,2′-bipyridine), for which alternating ferro- and antiferromagnetic interactions are expected. To our knowledge, this constitutes the first example of such a chain for any metal. A communication paper with preliminary results for the title compound has recently been published.[20]

Table 1. Crystal Data and Structure Refinement for $[Mn(bipy)(N_3)_2$

chem formula	$C_{10}H_8MnN_8$	Z	2
fw	295.18	T, °C	25
space group	$P\bar{1}$ (No. 2)	λ, Å	0.710 69
a, Å	7.547(2)	ρ_{obsd}, g cm^{-3}	1.65(2)
b, Å	9.137(4)	ρ_{calcd}, g cm^{-3}	1.651
c, Å	9.960(4)	μ, cm^{-1}	11.1
α, deg	110.76(4)	$R(F_o)^a$	0.055
β, deg	104.43(2)	$R_w(F_o^2)^b$	0.125
γ, deg	100.41(3)	S	0.964
V, Å^3	593.9(4)		

^{a} $R(F_o) = [\sum|\Delta F|/\sum|F_o|]$. ^{b} $R_w(F_o^2) = [\sum\{w(\Delta F^2)^2\}/\sum\{w(F_o^2)^2\}]^{1/2}$. The final difference $\rho_{max}{}^+/\rho_{max}{}^-$ (e/Å^{-3}) were +0.620/−0.610.

In this work, we present the crystal structure and spectroscopic and magnetic properties for the $[Mn(N_3)_2(bipy)]_n$ (bipy = 2,2′-bipyridine) compound. A theoretical model for a ferromagnetic−antiferromagnetic $S = {}^5/_2$ chain is described. The exchange interactions between the manganese(II) cations through the di-(μ-(end-on)azido) and di-(μ-(end-to-end)azido) bridges are also analyzed.

Experimental Section

Synthesis. This compound was synthesized following the method indicated in ref 20, by mixing solutions of 2,2′-bipyridine (methanol), $Mn(ClO_4)_2{\cdot}6H_2O$ (water), and NaN_3 (water).

Crystal Structure Determination. A rhombohedral shaped crystal of approximate dimensions 0.25 × 0.22 × 0.32 mm was sealed on a capillary and used for data collection on an Enraf-Nonius CAD-4 diffractometer. Cell constants and an orientation matrix for data collection were obtained by least-squares refinement of the diffraction data from 25 reflections in the θ range of 8−13°. The experimental density was determined by a flotation method in a bromoform/chloroform mixture. The main crystal structure determination data were compiled in the previously published communication.[20] The structure was solved via the heavy-atom Patterson procedures (SHELXS 86[21]) and refined with the SHELX93[22] computer program, with scattering factors from ref 23. Final refinement of the obtained model led to convergence at $R(F_o) = 0.055$ and $R_w(F_o^2) = 0.125$. The goodness of fit was $S = 0.964$. Crystallographic data and processing parameters are given in Table 1. The final positional parameters are shown in Table 2. Further details of the crystal structure investigation are available as Supporting Information.

Physical Measurements. Fourier transform infrared spectroscopy on KBr pellets was performed on a Perkin-Elmer 1720X FT-IR instrument, in the 400−4000 cm^{-1} region. Magnetic susceptibilities of powdered samples were carried out in the temperature range 2−300 K using a SQUID SHE magnetometer, equipped with a helium continuous-flow cryostat. The experimental susceptibilities were corrected for the diamagnetism of the constituent atoms (Pascal tables). ESR spectra were recorded, on powdered samples at X-band frequency, with a Bruker E.S.P. 300 spectrometer, equipped with a standard OXFORD low-temperature device, calibrated by the NMR probe for the magnetic field, the frequency being measured by using a Hewlett-Packard 5352B microwave frequency counter.

Results and Discussion

Crystal Structure. Selected bond distances and angles for the title compound are compiled in Table 3. An ORTEP[24] drawing of the one-dimensional $[Mn(N_3)_2(bipy)]_n$ complex and a view of the unit cell are shown in Figures 1 and 2, respectively.

The crystal structure consists of chains of Mn(II) ions alternatively linked by two EO [Mn−N1,N1^I, 2.200(6), 2.276(6)

(8) Duggan, D. M.; Hendrickson, D. N. *Inorg. Chem.* **1973**, *12*, 2422.
(9) (a) Commarmond, J.; Plumere, P.; Lehn, J. M.; Agnus, Y.; Louis, R.; Weiss, R.; Kahn, O.; Morgenstern-Badarau, I. *J. Am. Chem. Soc.* **1982**, *104*, 6330. (b) Sikorav, R. E.; Bkouche-Waksman. I.; Kahn, O. *Inorg. Chem.* **1984**, *23*, 490.
(10) Cortés, R.; Pizarro, J. L.; Lezama, L.; Arriortua, M. I.; Rojo, T. *Inorg. Chem.* **1994**, *33*, 2697.
(11) Arriortua, M. I.; Cortés, R.; Lezama, L.; Rojo, T.; Soláns, X.; Font-Bardia, M. *Inorg. Chim. Acta* **1990**, *174*, 263.
(12) Arriortua, M. I.; Cortés, R.; Mesa, J. L.; Lezama, L.; Rojo, T.; Villeneuve, G. *Transition Met. Chem.* **1987**, *13*, 371.
(13) (a) Rojo, T.; Lezama, L.; Cortés, R.; Mesa, J. L.; Arriortua, M. I.; Villeneuve, G. *J. Magn. Magn. Mater.* **1990**, *83*, 519. (b) Cortés, R.; Ruiz de Larramendi, J. I.; Lezama, L.; Rojo, T.; Urtiaga, M. K.; Arriortua, M. I. *J. Chem. Soc., Dalton Trans.* **1992**, 2723.
(14) (a) Vicente, R.; Escuer, A.; Ribas, J.; El Fallah, M. S.; Solans, X.; Font-Bardía, M. *Inorg. Chem.* **1993**, *32*, 1920. (b) Ribas, J.; Monfort, M.; Diaz, C.; Bastos, C.; Solans, X. *Inorg. Chem.* **1994**, *33*, 484. (c) Ribas, J.; Monfort, M.; Costa, R.; Solans, X. *Inorg. Chem.* **1993**, *32*, 695.
(15) (a) Ribas, J.; Monfort, M.; Diaz, C.; Bastos, C.; Solans, X. *Inorg. Chem.* **1993**, *32*, 3557. (b) Escuer, A.; Vicente, R.; El Fallah, M. S.; Ribas, J.; Solans, X.; Font-Bardia, M. *J. Chem. Soc., Dalton Trans.* **1993**, 2975. (c) Escuer, A.; Vicente, R.; Ribas, J.; El Fallah, M. S.; Solans, X.; Font-Bardía, M. *Inorg. Chem.* **1993**, *32*, 3727. (d) Cortés, R.; Urtiaga, M. K.; Lezama, L.; Pizarro, J. L.; Goñi, A.; Arriortua, M. I.; Rojo, T. *Inorg. Chem.* **1994**, *33*, 4009.
(16) Ribas, J.; Monfort, M.; Solans, X.; Drillon, M. *Inorg. Chem.* **1994**, *33*, 742.
(17) Cortés, R.; Urtiaga, M. K.; Lezama, L.; Ruiz de Larramendi, J. I.; Arriortua, M. I.; Rojo, T. *J. Chem. Soc., Dalton Trans.* **1993**, 3685 and references cited therein.
(18) Gregson, A. K.; Moxon, N. T. *Inorg. Chem.* **1982**, *21*, 586.
(19) Bencini, A.; Ghilardi, C. A.; Modollini, S.; Orlandini, A. *Inorg. Chem.* **1989**, *28*, 1958.
(20) Cortés, R.; Lezama, L.; Pizarro, J. L.; Arriortua, M. I.; Solans, X.; Rojo, T. *Angew. Chem., Int. Ed. Engl.* **1994**, *33*, 2488.
(21) Sheldrick, G. M. SHELXS86. *Acta Crystallogr.* **1990**, *A46*, 467.
(22) Sheldrick, G. M. SHELX93. *J. Appl. Crystallogr.*, manuscript in preparation (1994).
(23) *International Tables for X-ray Crystallography*; Kynoch Press: Birmingham U.K., 1974; Vol. IV, pp 99 and 149.
(24) Johnson, C. K. *ORTEP*; Report ORNL-3794; Oak Ridge National Laboratory: Oak Ridge, TN, 1965.

Table 2. Atomic Coordinates ($\times 10^4$) and Equivalent Isotropic Displacement Parameters ($A^2 \times 10^3$) for [Mn(bipy)(N_3)$_2$]

atom	*x*	*y*	*z*	*U*(eq)[a]
Mn	1174(1)	3966(1)	3874(1)	34(1)
N(1)	1181(8)	4792(7)	6237(6)	42(2)
N(2)	2590(9)	5239(7)	7327(7)	42(1)
N(3)	3877(10)	5605(10)	8374(8)	78(2)
N(4)	3486(9)	2793(8)	4340(7)	49(2)
N(5)	5107(9)	3366(6)	5095(6)	36(1)
N(6)	3288(9)	6124(8)	4147(7)	49(2)
N(7)	−1032(7)	1554(7)	3036(6)	34(1)
N(8)	189(8)	2792(7)	1297(6)	36(1)
C(1)	−1527(11)	912(10)	3966(9)	49(2)
C(2)	−2838(11)	−578(11)	3432(10)	51(2)
C(3)	−3702(11)	−1469(10)	1898(10)	54(2)
C(4)	−3248(10)	−839(9)	917(9)	45(2)
C(5)	−1898(9)	666(8)	1527(7)	33(2)
C(6)	−1257(9)	1438(8)	571(7)	34(2)
C(7)	−2104(11)	693(11)	−1016(8)	48(2)
C(8)	−1427(14)	1506(12)	−1830(9)	58(2)
C(9)	14(14)	2869(12)	−1087(10)	56(2)
C(10)	858(12)	3534(10)	487(9)	48(2)

[a] *U*(eq) is defined as one-third of the trace of the orthogonalized U_{ij} tensor.

Table 3. Bond Lengths (Å) and Angles (deg) for [Mn(bipy)(N_3)$_2$][a]

Mn−N6	2.185(6)	Mn−N1	2.200(6)
Mn−N7	2.237(5)	Mn−N4	2.244(6)
Mn−N8	2.258(5)	Mn−N1^{I}	2.276(6)
N1−Mn^{I}	2.276(6)		
N6−Mn−N1	98.8(2)	N6−Mn−N7	166.9(2)
N1−Mn−N7	94.3(2)	N6−Mn−N4	90.5(2)
N1−Mn−N4	92.3(2)	N7−Mn−N4	89.5(2)
N6−Mn−N8	95.3(2)	N1−Mn−N8	162.2(2)
N7−Mn−N8	71.7(2)	N4−Mn−N8	98.4(2)
N6−Mn−N1^{I}	92.2(2)	N1−Mn−N1^{I}	79.0(2)
N7−Mn−N1^{I}	89.8(2)	N4−Mn−N1^{I}	171.2(2)
N8−Mn−N1^{I}	89.7(2)	N2−N1−Mn	123.9(4)
N2−N1−Mn^{I}	124.5(5)	Mn−N1−Mn^{I}	101.0(2)
N5−N4−Mn	131.1(5)	N6^{II}−N5−N4	177.1(6)
N5^{II}−N6−Mn	127.3(5)	C5−N7−Mn	119.0(4)
C1−N7−Mn	123.7(5)	C6−N8−Mn	117.8(4)
C10−N8−Mn	122.5(5)		

[a] Symmetry transformations used to generate equivalent atoms (indicated by superscript I or II): (I) $-x$, $1-y$, $1-z$; (II) $1-x$, $1-y$, $1-z$.

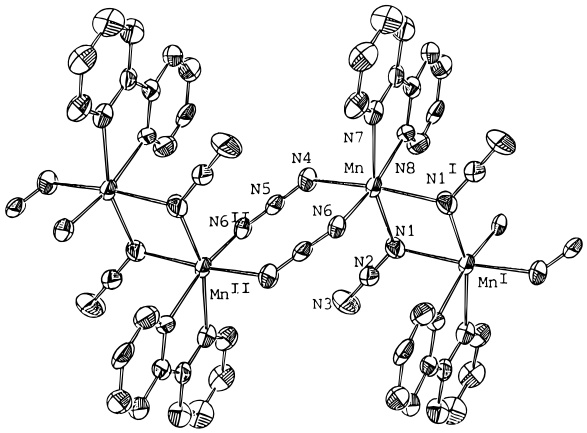

Figure 1. ORTEP view of the enchainment of [Mn(bipy)(N_3)$_2$] compound along the [100] direction, together with the atom labeling.

Å; I = $-x$, $1-y$, $1-z$] and two EE [Mn−N4,N6, 2.244(6), 2.185(6) Å] azido bridges (Figure 1). Each manganese(II) ion has a distorted octahedral coordination, completed by the two nitrogen atoms of the bipy ligand [Mn−N7,N8, 2.237(5), 2.258(5) Å]. Distortion of the coordination polyhedron around the Mn(II) from octahedral to trigonal prismatic has been

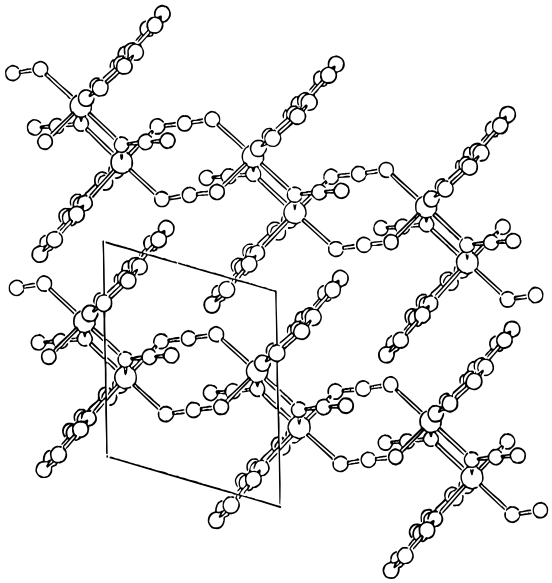

Figure 2. Arrangement of the chains in the *ab* plane.

calculated by the Muetterties and Guggenberger model.[25] The resulting value, $\Delta = 0.17$, indicates that the coordination polyhedron is close to octahedral geometry. The EO and EE bridges are arranged *cis*, being perpendicular to each other. The existence of an inversion center induces the Mn−N1−Mn^{I}−N1^{I} bridging unit to form a plane. The EO bridging azides, which are quasi-linear [N1−N2−N3, 176.6(8)°], slightly deviate (up and down) from that plane. The Mn−N1−Mn^{I} angle in the EO mode is 101.0(2)° in good agreement with the results usually obtained for this kind of bridging. For the EE bridges the Mn−N4−N5 angle is 131.1(5)° and Mn−N6−N5^{II} is 127.3(5)° (II = $1-x$, $1-y$, $1-z$), for a chair configuration of the Mn−(N_3)$_2$−Mn unit and a torsion angle of 41.9°. The intrachain Mn···Mn distances are 3.455(6) and 5.343(5) Å in the EO and EE bridges, respectively.

The bipy ligand can be considered as practically planar, with maximum deviations of −0.072 for C8 and +0.081 for C10. The bipy ligands stack parallel to each other (see Figure 2). An overlap between pairs of these ligands from two neighbor chains can be observed. These pairs are separated by approximately 3.5 Å, which allows the existence of $\pi-\pi$ interactions through bipy ligands.

Infrared Spectroscopy. The major interest of IR spectra for the azido bridged compounds is centered in the bands corresponding to the azido groups. There is not a great deal of information concerning the IR bands and its relationship with the structural data. So, correlations of this kind may be helpful in interpreting and rationalizing the absorption bands associated with every kind of azido bridge. In this way, selected bands of the title compound[26−28] and related ones with EO and EE coordination modes are compiled, in Table 4, for comparison.

The $\nu_{asym}(N_3)$ mode normally appears as a very strong band in the range 2000−2100 cm^{-1}. This band appears at about 2060 and 2100 cm^{-1} for the EO and EE bridging modes, respectively. Both frequencies are higher than those corresponding to the terminal azido group. The change from EO to EE coordination modes results in both an increasing in the frequency and a

(25) Muetterties, E. L.; Guggenberger, G. *J. Am. Chem. Soc.* **1974**, *96*, 1748.
(26) Cortés, R.; Lezama, L.; Larramendi, J. I. R.; Insausti, M.; Folgado, J. V.; Madariaga, G.; Rojo, T. *J. Chem. Soc., Dalton Trans.* **1994**, 2573.
(27) Tandon, S. S.; Thompson, L. K.; Manuel, M. E.; Bridson, J. N. *Inorg. Chem.* **1994**, *33*, 5555.
(28) Mautner, F. A. To be published.

Table 4. Selected Infrared Bands Corresponding to the Different Bridging Modes of the Azido Group in the Title and Some Related Compounds[a]

compound	bidging mode	ν_{as} (cm^{-1})	ν_s (cm^{-1})	δ (cm^{-1})	ref
$[Ni(terpy)(N_3)_2]_2 \cdot 2H_2O$	EO	2050	1305	615, 600	11
$[Cu,Ni(terpy)(N_3)_2]_2 \cdot 2H_2O$	EO	2060	1300	615, 600	26
$[Cu(2Bzpy)(N_3)_2]_2$	EO	2058			27
$[Ni(pepci)(N_3)_2]_2$	EO	2050	1300	620, 605	13b
$[Mn(terpy)(N_3)_2]_2 \cdot 2H_2O$	EO	2075	1300	615, 605	10
$N(CH_3)_4[Mn(N_3)_3]$	EE	2110, 2020	−	620, 610	28
$[Mn(bipy)_2(N_3)]_2(ClO_4)_2$	EE	2100, 2050	−	615, 600	unpublished
$[Ni(bipy)_2(N_3)]_n(ClO_4)_n$	EE	2060, 2040, 2010	1345[b]	615, 600	15d
$[Mn(bipy)(N_3)_2]_n$	EO, EE	2105, 2095, 2050	1325	615, 605	this work

[a] Abbreviations: terpy = 2,2′:6′,2″-terpyridine; 2Bzpy = 2-benzyl-pyridine; pepci = *N*′-(2-pyridin-2-ylethyl)pyridine-2-carbaldimine; bipy = 2,2′-bipiridine; EO = end-on; EE = end-to-end. [b] Very weak.

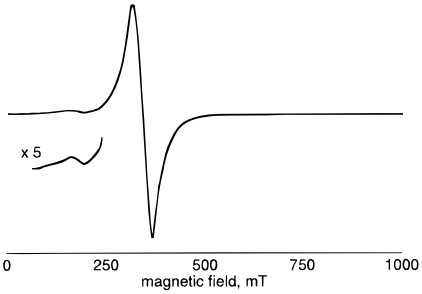

Figure 3. Room temperature ESR spectrum of $[Mn(bipy)(N_3)_2]$ compound.

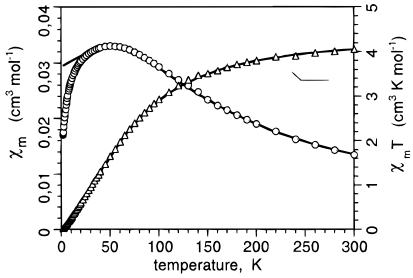

Figure 4. Thermal variations of the magnetic susceptibility (χ_m) and $\chi_m T$ product for $[Mn(bipy)(N_3)_2]$. The solid line represents the best fit curve according to the developed model.

splitting of this band. In the same way, an increase in the splitting can be observed when both the asymmetry of the EE bridge and the dimensionality of the compound are growing up (see Table 4). In the title compound, the ν_{asym} band is split with components at 2105, 2095, 2050, and 2010 cm^{-1}, which is consistent with a chain structure containing both end-on and end-to-end bridging ligands.

The azide symmetric stretch, $\nu_{sym}(N_3)$, appears at about 1300 cm^{-1} in the compounds with the EO bridging mode. This band is not active for the symmetrical EE coordination mode. The presence of a very weak (vw) band in this region for $[Ni(bipy)_2(N_3)]_n(ClO_4)_n$[15d] can be attributed to the asymmetry of the EE bridges in the complex. For the title compound, it appears at 1325 cm^{-1} due to the presence of EO bridges in the structure.

Finally, the band corresponding to the deformation mode (δ) of the azido group can be observed split in the region 600−625 cm^{-1} for all polynuclear compounds.

ESR and Magnetic Measurements. The X-band ESR spectrum of the title compound is shown in Figure 3.

ESR measurements show an exchange-narrowed isotropic signal at $g = 2.0$, which is indicative of significant ferromagnetic interactions. This signal does not significantly change with temperature. Further, a "half-field" signal can be observed associated with the $\Delta Ms = 2$ forbidden transition.

Variable-temperature magnetic susceptibility measurements, performed on a powdered sample from 298 to 2 K, are shown in Figure 4. The χ_m value increases upon cooling, reaching a rounded maximum at about 55 K, and then drops to zero at lower temperatures. The $\chi_m T$ value at room temperature is 4.05 cm^3 K mol^{-1}, which is smaller than the expected one for an uncoupled Mn(II) ion. This value decreases continuously upon cooling. According to the structural data, this compound should exhibit alternating ferro- and antiferromagnetic interactions. Indeed, the double EO bridges mediate ferromagnetic interactions between Mn(II) centers (as observed in the $[Mn(N_3)_2(terpy)]_2 \cdot 2H_2O$ dinuclear complex[10] with Mn−N−Mn^I 104.6(2)° and $J/k = +3.5$ K), while the double EE bridges with M−N−N $\approx$ 130° (the average angle in the title compound is 129.2°) promote antiferromagnetic coupling.[15a] As a result, the magnetic behavior of the title compound must be explained by assuming two alternating exchange constants: a positive J_1 for EO and a negative J_2 for EE pathways. A theoretical model for the alternating ferromagnetic−antiferromagnetic $S = {}^5/_2$ chain is proposed hereafter.

Theoretical Approach

Owing to structural findings, we consider in what follows the alternating chain with nearest neighbor exchange interactions described by the spin Hamiltonian

$$H = -J_1 \sum S_{2i} S_{2i+1} - J_2 \sum S_{2i+1} S_{2i+2}$$

where J_1 and J_2 stand for the alternating exchange constants, and the S's are classical spin operators. This approximation is justified for manganese(II) ion, which exhibits a large spin ($S = {}^5/_2$).

It is well-known that the wave vector dependent susceptibility is given by[29]

$$S(q) = \frac{1}{NkT} \sum_{n,p} \langle S_n S_{n+p} \rangle \exp(iqp)$$

which appears to be related to the pair correlation function between operators located at sites n and $n + p$, namely,

$$\langle S_n S_{n+p} \rangle = \frac{3}{Z} \int \frac{dS_1\, dS_2 \ldots dS_{N+1}}{(4\pi)^{N+1}} S_n{}^z S_{n+p}{}^z \exp(-H/kT)$$

In the limit of the uniform chain ($J_1 = J_2$), Fisher has shown, by expanding $\exp(-H/kT)$ in terms of spherical harmonics, that the above expression reduces to

$$\langle S_n S_{n+p} \rangle = (\coth(J/kT) - kT/J)^p = u^p$$

For the alternating chain, this formalism goes through, except that the pair correlation function now becomes

$$\langle S_n S_{n+p} \rangle = u_1 u_2 u_1 u_2 ...$$

with $u_1 = \coth(J_1/kT) - kT/J_1$ and $u_2 = \coth(J_2/kT) - kT/J_2$. Taking into account the p parity, we can write

$$S(q) = \frac{1}{kT}\{\sum_r {u_1}^{|r|}{u_2}^{|r|} \exp(2iqra) + ({u_1}^{|r+1|}{u_2}^{|r|} + {u_1}^{|r|}{u_2}^{|r+1|}) \exp(iq(2r+1)a)\}$$

By expanding the summation over integer r values, we obtain the wave-vector-dependent susceptibility in the quasi-elastic approximation

$$S(q) = \frac{1}{kT}\left(\frac{1 - {u_1}^2{u_2}^2 + (u_1 + u_2)(1 + u_1u_2)\cos(qa)}{1 - 2u_1u_2\cos(2qa) + {u_1}^2{u_2}^2}\right)$$

Then, we deduce the expression of the bulk susceptibility corresponding to the $q = 0$ limit

$$\chi = \frac{Ng^2{\mu_B}^2}{3kT}\left(\frac{1 + u_1 + u_2 + u_1u_2}{1 - u_1u_2}\right)$$

This expression reduces to the classical dimer and uniform chain limits[30] when u_1(or u_2) $= 0$ and $u_1 = u_2$, respectively.

Discussion of the Results. A close examination of the magnetic results, plotted in Figure 4 as χ_m and $\chi_m T$ vs T, reveals an antiferromagnetic low-dimensional behavior with significant couplings between manganese(II) ions, deduced from the large maximum around 50 K.

In order to make quantitative comparison with the theoretical expression deduced in the classical limit, we used the following scaling factors:

$$J_i \rightarrow J_i S(S+1)$$

$$g \rightarrow g(S(S+1))^{1/2}$$

Except in the dimer limit (u_1 or $u_2 = 0$), the chain model proposed above cannot explain the very low temperature behavior, since a nonzero value of the susceptibility is expected at absolute zero. Nevertheless, a fit of the experimental data was performed using the set of parameters (J_1, J_2, g). Clearly, a good agreement between theory and experiment is obtained when both interactions have opposite signs, only. Allowing all the parameters to vary, an acceptable fit is obtained with the set of parameters $J_1 = 21.7$ K, $J_2 = -16.0$ K, $g = 1.92$. However, the low value of g obtained is quite unrealistic for a Mn(II) compound. Fixing g to the expected value $g = 2$ for manganese(II), the best agreement theory−experiment corresponds to the following parameters: $J_1 = +13.8$ K, $J_2 = -17.01$ K.

The model proposed appears to provide a very good description of the susceptibility down to around 20 K. In the range 20−300 K, the discrepancy does not exceed the experimental uncertainty.

At very low temperature, the agreement is not so satisfactory, due probably to the influence of small interchain interactions, always present in those kinds of compounds. Considering the structural results, the existence of such interchain interactions can be explained by considering the overlap between bipy ligands belonging to adjacent chains (see Figure 2). These ligands are separated from each other by approximately 3.4 Å, and their planes are parallel, making the existence of $\pi-\pi$ interactions available.

Chart 1

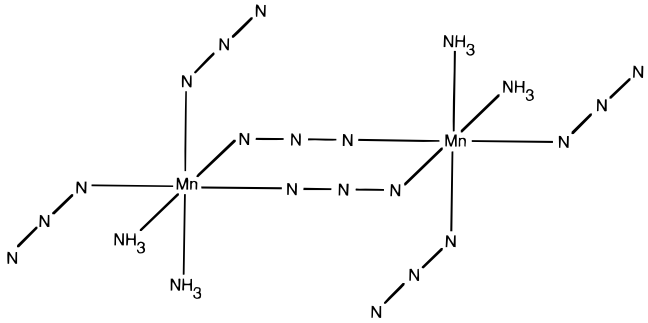

These results call for the following comments:

(i) The very good description of the experiment over a wide range of temperature shows that a classical treatment, renormalized to quantum spins, gives a satisfying picture of the alternating manganese(II) chain.

(ii) The alternating ferro- and antiferromagnetic interactions along the chain can be explained by considering the different exchange pathways. Thus, the EO azido bridge promotes, for a bridging angle of 101°, a ferromagnetic interaction, while the EE bridge gives rise to antiferromagnetic interaction.

(iii) At very low temperature, the variation of the experimental susceptibility indicates that interchain interactions take place. Further investigations, such as specific heat measurements would be required to conclude about the nature of the ground state.

Molecular Orbital Calculations. In order to analyze magnetostructural correlations for the title compound, Extended Hückel molecular orbital (EHMO) calculations[31] were performed on independent modelized EO and EE fragments. The atomic parameters used for Mn, N, and H were the standard of the program.

The exchange parameter can be viewed as the sum of antiferromagnetic (J_{AF}) and ferromagnetic (J_F) contributions, which depend on the splitting of the pairs of MO's (Δ), and the two-electron integrals, respectively. Only when J_{AF} is zero or negligible is the ferromagnetic behavior, J_F, predominant. The antiferromagnetic contribution can be analyzed as a function of the square of the gap (Δ^2) between the pairs of MO's derived from magnetic orbitals. Then, EHMO calculations are able to analyze the existing gap and therefore the antiferromagnetic component. In the title compound, alternating end-on and end-to-end azido bridges are present, so alternating ferro- and antiferromagnetic interactions are expected. In this way, for both modeled systems ten molecular orbitals are generated from the five magnetic orbitals, with one electron each, corresponding to the two Mn(II) ions. In this sense, the antiferromagnetic contribution should be proportional to the sum $\sum\Delta^2 = \Delta^2(d_{x^2y^2}) + \Delta^2(d_{z^2}) + \Delta^2(d_{xz}) + \Delta^2(d_{xy}) + \Delta^2(d_{yz})$. However, priority to the orbitals mainly implicated in the exchange pathway has been given in each modeled system.

For the EE azido fragment, three variable parameters must be investigated: (a) Mn−N(azide) distances, usually asymmetric; (b) Mn−N−N and N−N−Mn angles, also asymmetric; (c) dihedral angle, δ, between the bridging azides least squares plane and the N−Mn−N plane. The modelized Mn(II) end-to-end azido fragment is shown in Chart 1. The manganese(II) ions have been placed in a slightly distorted octahedral

(29) Thorpe, M. F. *J. Phys.* **1975**, *36*, 1177.
(30) (a) Fisher, M. E. *Am. J. Phys.* **1974**, *32*, 241. (b) Drillon, M.; Coronado, E.; Beltrán, D.; Georges, R. *Chem. Phys.* **1983**, *79*, 449.
(31) Mealli, C.; Proserpio, D. M. *Computer Aided Composition of Atomic Orbitals* (CACAO Program); PC version, July 1992 (kindly supplied by C. Mealli). See also: *J. Chem. Educ.* **1990**, *67*, 399.

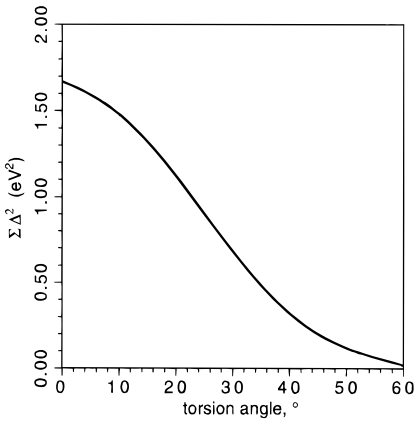

Figure 5. Variation of the square gap (Δ^2) as a function of the torsion angle for the end-to-end model.

environment. The N−Mn−N angle was taken as 90°, and the bond distances of Mn−N(NH_3) and Mn−N(azide) were 2.15 and 2.20 Å, respectively, which are similar to the values observed in the structure. In order to study the influence of the dihedral angle variation, the Mn(II) ions are allowed to rotate freely around the two terminal N atoms of the two azido bridging ligands.

In order to consider the effect of asymmetry of the Mn−N distances and Mn−N−N angles, EHMO calculations have been carried out for $\delta = 0$. Both the angles and distances have been varied in an asymmetrical form to allow for the existence of an inversion center as observed in the title compound. Only a great distortion in both bond angles and distances would be necessary to observe a variation of the magnetic behavior.

Another parameter to be considered is the dihedral angle (δ). A variation of this torsion angle from 0 to 60° has been carried out, and the results are shown in Figure 5. This range is used because larger angles seem to be sterically hindered. As can be seen, there is a large decrease in the J ($\approx\Delta^2$) value upon ranging the dihedral angle from 0 to 60°, which is practically zero for this last angle. So, as the dihedral angle in the title compound is 41.5°, a large value for the J_{AF} parameter should not be expected.

Considering these results, we can deduce that the variation of both the bond distance and angle parameters is negligible with respect to the torsion angle variation, which represents the driving parameter in the magnitude of the antiferromagnetic interaction.

In the case of end-on (EO) azido bridges, although EHMO calculations are not valid for analyzing the ferromagnetic component, they can be used to evaluate the antiferromagnetic contribution. So, we have performed calculations on a modelized hexacoordinate Mn(II) end-on-azido fragment, as shown in Chart 2.

Chart 2

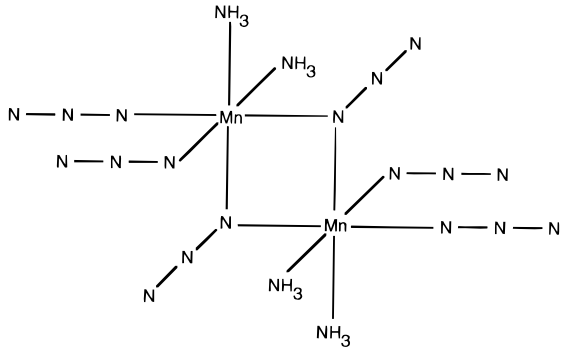

The influence of both the bridging angle and the asymmetry of the metal-bridge bonds has been analyzed (Figure 6). A decrease of the antiferromagnetic contribution is observed as the asymmetry of the bonds is raised. With respect to the bridging angle, care must be taken in selecting the magnetic orbitals used in the study. If all five magnetic orbitals are considered, a continuous decrease of the antiferromagnetic contribution appears as the bridging angle is raised, which seems to be unrealistic. However, considering the contribution of the magnetic orbital which is mainly implicated in the exchange pathway, the d_{yz} orbital (see Chart 2), a situation of accidental orthogonality is observed for a bridging angle of 105°.

Cu(II) and Ni(II) dimers with EO bridging mode[8,11,13,32] have shown that ferromagnetic interactions depend, to a large extent, on the value of the bridging M−N(azide)−M angles. For copper(II) EO−azido dimers, a theoretical value of the bridging angle of 103° has been predicted for the accidental orthogonality to occur.[7,32] Experimental data for the nickel dimers indicate the same correlation with a bridging angle larger than 102°.[13b] For those EO azido systems ferromagnetism is found to dominate, even for bridging angles differing from the accidental orthogonality.

Spin polarization theory[7] has been recurrently used to explain the ferromagnetic interactions observed in the end-on bridged azido systems. However, it has recently been demonstrated[33] that in the case of copper dimers with this kind of bridging ferromagnetic behavior prevails at small bridging angles (<108°) and that at larger angles antiferromagnetic exchange predominates. The spin polarization theory is therefore to be considered

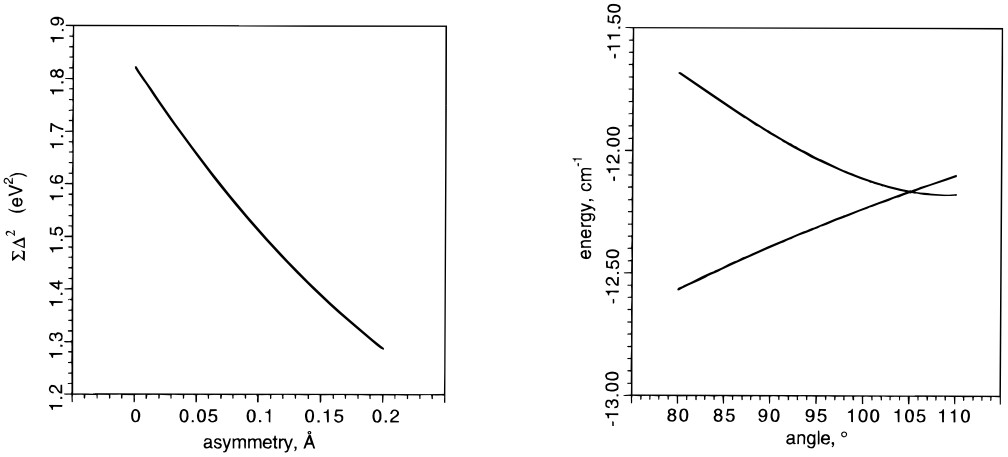

Figure 6. Variation of the square gap (Δ^2) as a function of the asymmetry of the bridging bonds (left), and variation of the energy for the d_{yz} orbitals as a function of the bridging angle (right) for the end-on model.

with caution, and, in fact, it may not be an appropriate description. In this way, a recent report[34] of a polarized neutron diffraction study on [Cu_2(*t*-bupy)$_4$(μ_2-1,1-N_3)](ClO_4)$_2$ revealed spin density calculations that contradict the theoretical interpretation involving spin polarization theory. Considering this situation, more complexes of this kind, showing different bridging angle values, should be necessary to thoroughly explain this interesting behavior.

Concluding Remarks

A synthetic method has successfully been employed to obtain a new manganese(II) one-dimensional compound containing alternating two end-on and two end-to-end azido bridges. The compound shows very scarce alternating ferro- (through EO bridges) and antiferromagnetic (through EE bridges) interactions, with a predominance of the antiferromagnetic component. Small interchain interactions are probably responsible of the very low temperature behavior.

A theoretical model has been developed to describe the magnetic behavior of the title compound. A good agreement between theory and experiment is obtained showing that a satisfying picture of the alternating $S = {}^5/_2$ one-dimensional system with a classical spin model is available. In order to study the magnetostructural correlations, extended Hückel MO calculations have been carried out for modelized EE and EO fragments. The torsion angle (δ) has been shown to be the driving parameter correlating the magnitude of antiferromagnetism for the EE coordination mode. The larger is the torsion angle, the weaker are the antiferromagnetic interactions. In the case of compounds with the EO bridges, the magnitude of the antiferromagnetic component decreases with the asymmetry of the bridging bonds, while an accidental orthogonality is observed for the variation of the bridging angle. According to recent reports, the driving effect for magnetic interactions through this kind of bridge seems to be the value of the bridging angle. Ferromagnetic interactions would prevail at small angles, while angles larger than approximately 108° would let the existence of antiferromagnetic interactions.

Acknowledgment. We are very grateful for a grant-in-aid for Scientific Research from the Universidad del Pais Vasco/Euskal Herriko Unibertsitatea (UPV/EHU 130.310.EB234/95).

Supporting Information Available: Listings of structural determinations, anisotropic displacement parameters, hydrogen atom coordinates, bond distances and angles, and torsion angles (10 pages). Ordering information is given on any current masthead page.

IC961017E

(32) Kahn, O.; Sikorav, S.; Gouteron, J.; Jeannin, S.; Jeannin, Y. *Inorg. Chem.* **1983**, *22*, 2877.
(33) Thompson, L. K.; Tandon, S. S.; Manuel, M. E. *Inorg. Chem.* **1995**, *34*, 2356.
(34) Aebersold, M.; Bergerat, P.; Gillon, B.; Kahn, O.; Pardi, L.; Tukzet, F.; Öhrström, L.; Grand, A. *NATO Advanced Research Workshop on Magnetism-A Supramolecular Function*; Carcans-Maubuisson, France, Sept 16−21, 1995.